Made available through Montana State University's ScholarWorks

In C57BL/6J mice, weight loss in previously obese mice reduced bone mass and shifted the cortical bone metabolome

Carolyn Chlebek, Casey McAndrews, Benjamin Aaronson, Hope D. Welhaven, Kanglun Yu, Samantha Costa, Joseph R. Shaver, Sophia Silvia, Victoria DeMambro, Ronald K. June, Meghan E. McGee‐Lawrence, Clifford J. Rosen

Accessibility Disclaimer:

For a more accessible version of this document, please submit an accessibility request form through the Montana State University Library website.

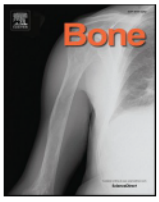
Bone 202 (2026) 117690



Contents lists available at ScienceDirect

Bone

journal homepage: www.elsevier.com/locate/bone



Full Length Article



In C57BL/6J mice, weight loss in previously obese mice reduced bone mass and shifted the cortical bone metabolome

Carolyn Chlebek [a,*], Casey McAndrews [b], Benjamin Aaronson [b], Hope D. Welhaven [c,d], Kanglun Yu [e], Samantha N. Costa [a,f], Joseph Shaver [e], Sophia Silvia [b], Victoria E. DeMambro [a,f], Ronald K. June [g,h], Meghan E. McGee-Lawrence [e], Clifford J. Rosen [a,f,i]

[a] Center for Molecular Medicine, MaineHealth Institute for Research, Scarborough, ME, USA
[b] University of New England College of Osteopathic Medicine, Biddeford, ME, USA
[c] Department of Chemistry and Biochemistry, Montana State University, Bozeman, MT, USA
[d] Molecular Biosciences Program, Montana State University, Bozeman, MT, USA
[e] Department of Cellular Biology and Anatomy, Medical College of Georgia, Augusta University, Augusta, GA, USA
[f] Graduate School of Biomedical Sciences and Engineering, University of Maine, Orono, ME, USA
[g] Department of Mechanical and Industrial Engineering, Montana State University, Bozeman, MT, USA
[h] Department of Microbiology and Cell Biology, Montana State University, Bozeman, MT, USA
[i] School of Medicine, Tufts University, Boston, MA, USA

ARTICLE INFO

Keywords:
Nutrition
Preclinical studies
Bone-fat interactions
Other – diseases and disorders of/related to bone
Bone QCT/microCT
DXA
Molecular pathways - remodeling

ABSTRACT

Obesity is linked to increased fracture risk. Despite the negative effects of weight loss on the skeleton, patients with obesity are advised to lose weight via calorie restriction. Obesity and weight loss individually alter both whole-body and local metabolism. Little is known about changes to bone mass and metabolome following calorie restriction in obese preclinical models. We hypothesized that caloric restriction would reduce bone mass in obese mice and would alter the cortical bone metabolome. To induce obesity, 8-week-old male and female C57BL/6J mice received 60 % kCal high-fat diet for 12 weeks. From 20 to 30 weeks of age, mice either remained obese or lost weight through 30 % caloric restriction. Controls consumed 10 % kCal low-fat diet. Compared to obesity, calorie restriction elicited cortical bone loss and trabecular thinning. Weight loss also reduced bone formation. Both obesity and subsequent calorie restriction altered the cortical bone metabolome in a sex-dependent manner. Metabolic pathways altered with diet generally mapped to amino acid or fatty acid metabolism. In males, weight loss was associated with a downregulation of pathways related to tryptophan, tyrosine, ubiquinone, and fatty acids. In females, calorie restriction downregulated taurine and hypotaurine metabolism but upregulated pyrimidine metabolism, nicotinate and nicotinamide metabolism, and pantothenate and CoA biosynthesis. In summary, despite improvements in components of systemic metabolism, caloric restriction in obese preclinical models reduced bone mass and did not restore the cortical metabolome to control conditions.

1. Introduction

Obesity is associated with a wide range of negative health outcomes, including increased fracture risk [1,2]. The number of patients diagnosed with obesity in the United States is rising [3], which will lead to more fractures and add to the healthcare burden. In addition to increased fracture risk, patients with obesity are more likely to be diagnosed with advanced osteoarthritis, requiring surgical intervention [4]. Total hip and total knee replacements are common procedures used to improve pain-related symptoms and mobility. These surgeries rely on osseointegration, or the ingrowth of both cortical and trabecular bone onto the implant surface [5], and thus bone quality may affect surgical outcomes, particularly in patients with obesity. Weight loss is often recommended for patients with obesity and can be achieved via a calorie-restricted diet, exercise, anti-obesity medications, or bariatric surgery. Due to the noninvasive nature of lifestyle interventions, diets such as calorie restriction are often first-line clinical recommendations for weight loss [6].

Diet-induced obesity in the mouse elicits skeletal changes that mirror clinical findings and thus serve as a useful model of obesity. In high-fat

* Corresponding author at: MaineHealth Institute for Research, 81 Research Drive, Scarborough, ME, 04074, USA.
E-mail address: carolyn.chlebek@mainehealth.org (C. Chlebek).

https://doi.org/10.1016/j.bone.2025.117690
Received 18 July 2025; Received in revised form 15 October 2025; Accepted 22 October 2025
Available online 27 October 2025
8756-3282/© 2025 The Authors. Published by Elsevier Inc. This is an open access article under the CC BY license (http://creativecommons.org/licenses/by/4.0/).

diet-fed mice, trabecular bone morphology is negatively altered, with obesity-induced reductions in bone volume fraction and trabecular number [7–9]. Cortical thickness also is decreased by obesity, with fewer morphological changes than trabecular bone [7,8]. In humans, although obesity is generally associated with increased bone mineral density [2], body fat percentage is negatively correlated with cortical bone mass and mechanical properties [10,11]. Additionally, in humans and mice, obesity increases bone marrow adipose tissue accumulation [9,12,13], which is negatively correlated with skeletal health [13].

In the absence of obesity, calorie restriction has been linked to bone loss, both clinically and in rodent models. When calories are restricted in individuals without obesity, bone mineral density is reduced [14,15]. In postmenopausal women, weight loss was associated with more rapid age-related declines in bone microarchitecture in both the cortical and trabecular envelopes [16]. Similarly, in nonobese mice, calorie restriction decreases cortical bone mass and suppresses bone formation [17–21]. The effect of calorie restriction on trabecular bone is less clear; some studies report that trabecular bone is negatively affected by caloric restriction [17,18] whereas other researchers report improved trabecular bone morphology [19–21]. Paradoxically, bone marrow adipose tissue is increased by calorie restriction in nonobese murine models [18,21] and following weight loss in nonobese humans [22,23].

Research investigating the effect of weight loss on the skeleton after obesity is limited. In humans with obesity, following weight loss, bone mineral density is increased in males but decreased in females [24]; however, high body mass index is associated with lower precision with regards to bone mineral density evaluated by dual-energy x-ray absorptiometry [25,26]. In preclinical models, obese mice that were transitioned from a high- to low-fat diet lost weight, but the effects of diet change on bone quality were sex-dependent [9,27]. Following weight loss with a low-fat diet, formerly obese mice retained obesity-induced skeletal deficits [9,27].

Both obesity and weight loss are associated with shifts in whole-body and local metabolism. Obesity increases circulating glucose levels and negatively affects insulin-stimulated glucose uptake in several organs, including the bone marrow [28]. When obese individuals lose weight, fasting blood glucose is reduced and insulin sensitivity increased [29]. Interestingly, circulating metabolites also shift in obese individuals who alter their diet to achieve weight loss [30]. In addition to whole-body metabolic changes elicited by obesity and subsequent weight loss, cellular metabolism within bone cells is likely also affected. Mitochondrial dysfunction is evident when osteoblasts are differentiated in high glucose media, a method to simulate obesity in vitro [31]. Similarly, culturing osteocytes in high fatty acid or high glucose conditions reduces mitochondrial activity and increases cellular reactive oxygen species [32].

We sought to understand the skeletal changes following caloric restriction in obese preclinical models. We hypothesized that caloric restriction would worsen bone quality in obese mice, independent of sex. Obesity-induced skeletal deficits were confirmed prior to weight loss, and components of whole-body metabolism were evaluated both during obesity and following caloric restriction. In addition to evaluating diet-induced changes to skeletal morphology and bone formation, we also investigated whether obesity and subsequent caloric restriction altered the cortical bone metabolome.

2. Materials and methods

2.1. Mice

Male and female C57BL/6J mice aged 5 weeks (Jackson Laboratories, Bar Harbor, ME) were acclimated for three weeks prior to the experiment. All mouse procedures were performed under the approval of the Institutional Animal Care and Use Committee (IACUC) at the MaineHealth Institute for Research. Throughout the study, mice were housed in 14-h light:10-h dark cycles. Outside of fasting periods, all animals had ad libitum access to food and water. Bodyweight was recorded at baseline and weekly thereafter. Sample sizes for micro-computed tomography were determined using a power analysis ($\alpha = 0.05$, $P = 0.80$) of cortical thickness in a previously published study [21]. Sample sizes for osteoblast and osteoclast number were determined using a power analysis ($\alpha = 0.05$, $P = 0.80$) of trabecular osteoblast and osteoclast number per bone perimeter in a previously published study [21].

2.2. Dual energy x-ray absorptiometry

Body mass, composition, bone mineral content (BMC), and bone mineral density (BMD) were measured at baseline and at the end of each diet phase using dual energy x-ray absorptiometry (Faxitron UltraFocus-DXA, Hologic, Marlborough, MA). Calibration was performed using phantom standards provided by the manufacturer. The mouse cranium was removed from analysis. Areal bone mineral content, bone mineral density, fat mass, percent fat, and lean mass were calculated.

2.3. Obesity induction

During the High Fat Feeding Phase, mice were housed in groups of two or three per cage. At 8 weeks of age, the High Fat Feeding Phase was initiated. Cages were randomly assigned to receive a 60 % high fat diet, containing 60 % of calories from fat ($n = 34$) or a 10 % kcal low fat diet, containing 10 % of calories from fat ($n = 18$) (D12492i and D12450Ji, respectively; Research Diets Inc., New Brunswick, NJ). Male mice received at least 3.5 g of diet per mouse per day; females had at least 3 g per mouse per day. Low fat diet consumption was evaluated weekly. High fat diet was completely replaced every 2–3 days.

Following 12 weeks of high- or low-fat feeding, mice were determined to be obese or nonobese by evaluating bodyweight, fat mass, and percent body fat (Fig. S1). Based on these criteria, seven female mice were excluded at the end of the High Fat Feeding Phase due to failure to become obese. To confirm the skeletal phenotype in mice at the end of the High Fat Feeding Phase, 5 mice per group were euthanized in both males and females. One male mouse was euthanized prior to the conclusion of the High Fat Feeding Phase due to a bad reaction to an insulin injection.

2.4. Weight loss induction

Following obesity induction, obese mice were randomly assigned to remain on the high fat diet (HFD) or were assigned to the diet-induced weight loss (HFD-CR). At the conclusion of the High Fat Feeding Phase, all mice were single housed. HFD animals continued to receive 60 % high fat diet. HFD-CR mice received the low fat diet for 2 weeks (Stabilization Phase) and were then transitioned to a 30 % calorie-restricted diet for 8 weeks (Caloric Restriction Phase) (Fig. 1A). All mice were euthanized at the end of the Caloric Restriction Phase, at 30 weeks of age.

When fed at 30 % restriction, the calorie restriction diet (D15032801i; Research Diets Inc., New Brunswick, NJ) contains equal amounts of vitamins and minerals to that consumed by control mice. Mice receiving a low fat diet during obesity induction remained on the same diet for the study duration (Control). Weekly food consumption in the control group was used to determine the amount of calorie restriction food for HFD-CR mice in the subsequent week. HFD-CR mice were fed within the same two-hour window each day. Two female HFD-CR mice were euthanized prior to the end of the study due to lack of food consumption during the Stabilization Phase. An additional two female mice were euthanized due to dermatitis.

2.5. Glucose and insulin tolerance testing

Glucose and insulin tolerance were assessed at the end of the High

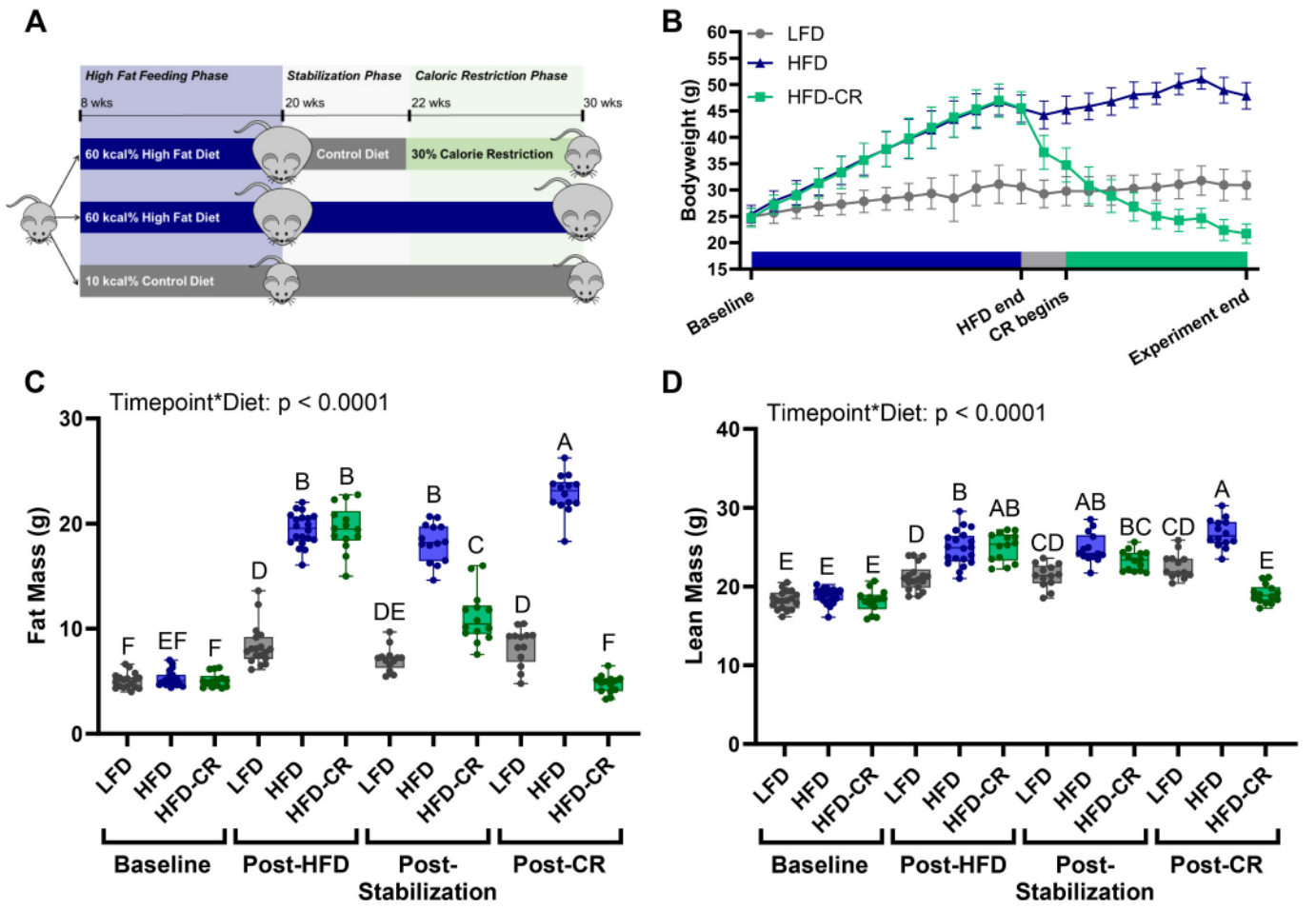


Fig. 1. Body mass increased during high fat feeding and decreased during caloric restriction. (A) Obesity was induced in 8-week-old male and female mice with a diet containing 60 % kcal from fat (HFD) during the High Fat Feeding Phase. After 12 weeks of high fat feeding, mice meeting the obesity criteria were randomly assigned to lose weight with caloric restriction or remain obese. To induce weight loss, animals were transitioned to a diet containing 10 % kcal from fat (LFD) for 2 weeks, followed by 8 weeks of caloric restriction. A final control group received LFD for the duration of the experiment. (B) During the High Fat Feeding Phase, males receiving high fat diet gained bodyweight. During the Caloric Restriction Phase, calorie restricted mice lost weight. (C) Body scans were obtained at baseline and at the end of each diet phase using DXA. HFD increased fat mass, but stabilization reduced fat mass. Subsequent caloric restriction further decreased fat mass. (D) Lean mass was increased by HFD but decreased following caloric restriction. Fat and lean mass were analyzed by two-way ANOVA with factors of timepoint and diet. Significant interaction terms are displayed. Tukey post-hoc analysis determined differences between groups. $p \leq 0.05$ for all effects displayed. Letters denote statistical differences: A > B > C > D > E > F.

Fat Feeding and Caloric Restriction Phases. Starting in the morning, mice were fasted for 6 h with free access to water. Fasting blood glucose was then recorded (AlphaTrak 2, Zoetis, Parsippany-Troy Hills, NJ). Mice were then injected intraperitoneally with glucose (1 g/kg bodyweight) or insulin (1 U/kg bodyweight). Blood glucose was recorded at 15, 30, 45, 60 and 120 min following injection. For glucose tolerance tests, blood glucose was plotted over time. For insulin tolerance tests, blood glucose was first normalized to the fasting blood glucose and then plotted over time. Area under the curve was calculated.

2.6. Indirect calorimetry

One week prior to euthanasia, 8 animals from each group were housed in metabolic cages (Promethion cages, Sable Systems Intl., North Las Vegas, NV). Metabolic cages contained standard bedding, a food hopper, water bottle, a house-like enrichment tube for body mass measurements, and a 11.5 cm running wheel that recorded revolutions. Following a 24 h acclimation in the metabolic cages, data was collected for 72 h. Data was analyzed separately for day, night, and 24-h cycles. Promethion Live software (v23.0.5) was used for data acquisition and instrument control. Raw data was processed with Macro Interpreter (v22.10). Respiratory quotient and energy expenditure were determined by assessment of respiratory gases, using standard equations [20,33] (Promethion Core™ CCF, Sable Systems Intl.). Ambulatory activity and the position of each mouse was determined with XYZ beam arrays (beam spacing of 0.25 cm).

2.7. Adipose depot evaluation

At euthanasia, inguinal fat pads were collected and weighed. Tissues were then fixed in 10 % formalin for 48 h on an orbital shaker. Following fixation, adipose depots were transferred to 70 % ethanol. Inguinal fat pads from five mice per group were then sectioned and stained for hematoxylin and eosin. Adiposity was quantified in ImageJ (version 2.14.0/1.54f) using a region of interest measuring 263 μm^2. Adipocyte number and size were averaged across two sequential sections per animal [34].

2.8. Dynamic histomorphometry

Prior to euthanasia (−10 days, −3 days), mice received calcein injections (10 mg/kg). One tibia from each mouse was embedded in plastic and sectioned for dynamic histomorphometry. Cortical bone was sectioned in the transverse plane whereas trabecular bone was sectioned

in the coronal plane. A single user calculated bone surface, single labels, and double labels in a blinded fashion for cortical bone. A second user quantified bone surface, single labels, and double labels in trabecular bone. Measurements of mineral apposition rate (MAR), mineralized surface per bone surface (MS/BS), and bone formation rate (BFR/BS) were calculated for trabecular and cortical bone BioQuant (BIOQUANT OSTEO 2021, Nashville, TN). Cortical endosteal and periosteal surfaces were evaluated separately. For trabecular bone samples, the region of interest consisted of a 3 × 4 grid of 800 × 500 μm panels starting at the bottom of the growth plate, excluding anything within 200 μm of the cortical bone.

2.9. Micro-computed tomography

At euthanasia, one tibia per mouse was collected for micro-computed tomography (μCT). Bones were fixed in 10 % formalin and placed on a rocker for 24 h. Bones were then rinsed and transferred to 70 % ethanol, then stored at 4 °C. In accordance with the American Society for Bone and Mineral Research guidelines [35], all bones were scanned using the same instrument (vivaCT 40, Scanco Medical AG, Brüttisellen, Switzerland) under the same conditions. Scans were acquired using a 10.5 μm^3 isotropic voxel size, 70 kVp peak x-ray tube intensity, 114 mA x-ray tube current, and 250 ms integration time. All scans were subjected to Gaussian filtration and segmentation. All analyses were performed using the Scanco software.

2.10. Tibiae histology and immunohistochemistry

Following analysis with μCT, five bones per group were decalcified in 14 % EDTA for two weeks. Tibiae were then paraffin-embedded and sectioned sagittally at 5 μm thickness. Sections were stained for hematoxylin and eosin, TRAP (Sigma-Adrich 387A), or anti pro-collagen-1 specific antibodies (Developmental Studies Hybridoma Bank SP1·D8). In hematoxylin and eosin-stained sections, bone marrow adiposity was quantified in ImageJ using a region of interest beginning 200 um below the growth plate and extending 3000um into the marrow cavity. Using previously established methods [34], adipocyte number and size were averaged across two sequential sections per animal.

To evaluate osteoblast and osteoclast number, metaphyseal endocortical cortical bone surface and trabecular bone were analyzed separately ($n = 5$/group). Bone-lining, cuboidal cells stained by procollagen-1 were quantified and normalized to bone surface. Similarly, the number of TRAP-positive cells was normalized to the bone surface and quantified. The number of procollagen-1- or TRAP-positive cells were quantified in sequential sections per mouse and the average calculated. One animal was excluded from osteoblast quantification due to significant tears during sectioning that prohibited accurate measurements.

2.11. Serum collection and analysis

Following euthanasia, blood was collected and stored at 8 °C for 24 h. Samples were then centrifuged and serum collected and stored at −80 °C. Serum CTx and P1NP were measured by ELISA according to manufacturer's instructions (IDS AC-06F1 and IDS AC-33f1, Bolden Colliery, United Kingdom).

2.12. Metabolomics

At euthanasia, femurs were cleaned of soft tissues and periosteum. Bone marrow was removed via centrifugation from femurs in all animals. Trabecular bone was removed from the femur and the cortical shell flash frozen in liquid nitrogen. A subset of femurs collected at the end of the Caloric Restriction Phase were included for metabolomic analysis (Fig. S2). Using a bead mill, bone was pulverized in a 70:30 methanol:acetone solution. Samples were centrifuged and supernatant containing metabolites was extracted. Supernatant was then dried in vacuum concentrator. Metabolites were then resuspended in 1:1 acetonitrile:water. All solvents used were high-performance liquid chromatography grade.

Following metabolite extraction [36], samples were analyzed by untargeted liquid chromatography-mass spectrometry (LC-MS) using Waters I-Class Ultra-High Performance Liquid Chromatography coupled to a Waters Synapt-XS Q-IMS-TOF in positive mode (Waters, Milford, MA). A Cogent Diamond Hydride hydrophilic interaction liquid chromatography (HILIC) chromatography column was utilized (2.2 μM, 120 Å, 150 mm × 2.1 mm; MicroSolv, Leland, NC, USA). 5 μL of sample was injected and blank samples were analyzed every 10 samples for quality control to prevent spectral drift and contamination. LC-MS data was then exported and converted for analysis using Progenesis.

Metabolomic data was assessed with MetaboAnalyst [36]. Normalized abundances were log transformed, standardized and auto-scaled. For all metabolic analysis, male and female mice were analyzed separately. To determine whether largescale shifts in metabotype occurred following weight gain and weight loss, partial least squares-discriminant analysis was performed. To identify metabolic pathways altered by diet, HFD and HFD-CR metabolite intensities were normalized to the median intensity in LFD animals and hierarchical clustering performed. The metabolites comprising each cluster were then correlated to metabolic pathways using MetaboAnalyst's MS Peaks to Pathways feature with the *mummichog* algorithm.

2.13. Statistical analyses

For all measures, male and female mice were analyzed separately. Longitudinal data was analyzed using a two-way ANOVA with factors of diet and timepoint (bone mineral density, body composition). Tukey's post-hoc tests determined significant differences between groups. Glucose and insulin tolerance tests performed at the end of each diet phase were analyzed separately to avoid any confounding factors, such as differences in experimental handlers or room conditions. One-way ANOVA for diet was used to assess differences for area under the curve for glucose and insulin tolerance tests, as well as ambulatory data collected during metabolic cage housing. For energy expenditure data collected with indirect calorimetry, diet differences were determined with ANCOVA, to correct for differences lean mass.

To determine differences following obesity induction, *t*-tests were used in for the small cohort of euthanized animals (peripheral adipose depots, bone morphology, dynamic histomorphometry, osteoblast number, osteoclast number, marrow adiposity). Normality was assessed using the Shapiro-Wilk test. Data that was not normally distributed was then analyzed by the Mann-Whitney *U* test.

To determine differences following weight loss, data were analyzed using a one-way ANOVA for diet (bone morphology, dynamic histomorphometry, P1NP, osteoblast number, CTx, marrow adiposity). Tukey's post-hoc tests determined significant differences between groups. Normality was assessed using the Shapiro-Wilk test. Data that was not normally distributed was then analyzed by Kruskal-Wallis test with post-hoc analysis by Dunn's multiple comparisons test.

In all tests, significance was set at $p < 0.05$. All statistical analyses were performed in R.

3. Results

3.1. High fat diet and subsequent caloric restriction changed body composition and whole-body metabolism

Compared to LFD control animals, HFD and HFD-CR mice gained body weight and fat mass during high fat feeding (Fig. 1B). Caloric restriction reduced body weight and fat mass in HFD-CR compared to both HFD and LFD mice (Figs. 1B–C, S3A–B). Lean mass increased during high fat feeding and decreased with caloric restriction (Figs. 1D, S3C).

Diet altered both glucose and insulin tolerance. In both sexes, fasting

blood glucose was elevated by high fat feeding but reduced by caloric restriction (Fig. S4). Compared to control mice, glucose tolerance was worsened in HFD and HFD—CR mice after the High Fat Feeding Phase in both male and female mice (Fig. S5A). In both sexes, caloric restriction improved glucose tolerance in HFD-CR compared to both LFD and HFD animals (Fig. S5B). After high fat feeding, insulin tolerance was worsened in male mice, but not altered in females (Fig. S5C). By the end of the study, HFD females had worse insulin tolerance compared to LFD mice (Fig. S5D). Following caloric restriction, HFD-CR mice had improved insulin tolerance compared to both HFD and LFD mice, in both sexes (Fig. S5D).

Whole-body metabolism was further analyzed with indirect calorimetry. In male mice, after accounting for lean mass, energy expenditure did not vary between groups (Table S1). In females, daytime and 24-h energy expenditure were significantly higher in HFD compared to LFD mice, even after accounting for differences in lean mass. Compared to LFD, HFD females had reduced nighttime and 24-h respiratory exchange ratios. In both sexes, ambulatory patterns varied by diet. Calorie-restricted mice ran further and faster compared to both HFD and LFD animals (Fig. S6A). Compared to HFD animals, HFD-CR mice also walked further and faster within the cage (Fig. S6B). Walking distance did not vary between LFD and HFD-CR mice.

3.2. Diet altered the mass and adiposity of white inguinal adipose tissue

Adipose depots were evaluated in a small cohort of mice euthanized after the High Fat Feeding Phase and at the end of the Caloric Restriction Phase (Fig. 1A). In both male and female mice, inguinal fat pad weights increased with high fat feeding (Table S2, Fig. S7). Calorie restricted mice had smaller inguindal fat pad mass compared to HFD mice.

Obesity changed the adiposity of inguinal adipose depots. At the conclusion of the High Fat Feeding Phase, inguinal adipocytes were larger in obese animals compared to controls in both male and female mice (Table S2). Compared to HFD mice, HFD-CR animals had smaller adipocytes (Fig. S8). This increase in adipocyte size resulted in fewer adipocytes per area in HFD mice (Table S2, Fig. S8). In male mice, the percent area occupied by inguinal adipocytes was not altered by 12 weeks of high fat diet; conversely, obese females had a higher percent area occupied by adipocytes compared to LFD controls (Table S2). After the Caloric Restriction Phase, HFD mice had a higher percent area occupied by adipocytes compared to both LFD and HFD-CR (Fig. S8).

Adiposity of bone marrow adipose tissue was altered by diet regimen. Following the High Fat Feeding Phase, obesity increased the size of bone marrow adipocytes, but adiposity was not significantly increased (Table S2). Similarly, after the Caloric Restriction Phase, adipocytes in HFD mice were larger than LFD in both sexes (Fig. S9). Female HFD-CR mice also had larger adipocytes compared to LFD controls. In male mice, caloric restriction following HFD significantly increased adipocyte number compared to LFD. The percent area occupied by adipocytes was similarly increased in HFD-CR females versus LFD.

3.3. High fat feeding altered bone morphology and bone mineralization

After 12 weeks of high fat feeding, a small subset of mice was euthanized to confirm the skeletal changes induced by obesity. Compared to LFD mice, high fat feeding reduced cortical and trabecular thickness in males (Table S3). Obesity also reduced trabecular bone formation rate and mineralizing surface in male mice, though not statistically different in our small sample size ($p < 0.1$). In female mice, obese animals had more cortical area compared to LFD. Compared to LFD mice, HFD females had reduced periosteal bone formation and mineral apposition rates, though not statistically different in our small sample size ($p < 0.1$). In this small cohort, the number of TRAP- or Procollagen-1-positive cells on the trabecular and cortical surfaces did not differ between LFD and HFD mice after 12 weeks of high fat diet in either sex.

3.4. Calorie restriction reduced bone mass in previously obese mice

Changes in areal bone mineral density (aBMD) and bone mineral content (aBMC) were monitored at the end of each diet phase (Fig. S10). Both aBMD and aBMC increased in LFD mice during the High Fat Feeding Phase. Compared to baseline, male mice receiving HFD during the High Fat Feeding Phase had increased aBMC but not aBMD. Conversely, in females, aBMD was not different by diet regiment, but HFD mice had greater aBMC compared to LFD controls. Following the 2-week Stabilization Phase, HFD-CR males had increased aBMD compared to their obese counterparts. Following the Caloric Restriction Phase, compared to HFD males, HFD-CR mice retained increased aBMD. In both males and females, caloric restriction reduced aBMC compared to HFD mice.

Calorie restriction reduced cortical bone mass more than obesity alone (Fig. S11). At the end of the Caloric Restriction Phase, cortical area, thickness, and area fraction were reduced in HFD-CR mice compared to controls in both sexes (Fig. 2A–C). Compared to obese mice, calorie restriction increased marrow area and decreased the moment of inertia in females, but not males (Fig. 2D–E). Cortical tissue mineral density was not different between diet groups (Fig. 2F). In both sexes, caloric restriction reduced tibia length compared to obese mice (Fig. 2G). In females, total cortical area increased in HFD versus LFD mice, but did not change with HFD-CR. Total cortical area did not differ between diets in male mice.

Trabecular bone was altered by weight loss in both sexes (Fig. 3). In males, bone volume fraction was reduced in HFD-CR mice compared to LFD (Fig. 3A). Diet did not change trabecular bone volume fraction in females (Fig. 3A). Compared to HFD and LFD animals, HFD-CR mice had reduced trabecular thickness in both sexes (Fig. 3B). Compared to LFD, male HFD and HFD-CR mice had increased trabecular separation but reduced trabecular number (Fig. 3C–D). Female HFD had increased trabecular separation compared to LFD (Fig. 3C). In females, caloric restriction reduced trabecular separation and increased trabecular number in HFD-CR compared to HFD mice (Fig. 3C–D). Compared to LFD mice, HFD and HFD-CR reduced trabecular tissue mineral density in male mice (Fig. 3E). Diet did not change trabecular tissue mineral density in females (Fig. 3E).

3.5. Calorie restriction reduced bone formation in both male and female mice

Caloric restriction reduced bone formation in both the cortical and trabecular compartments. In both sexes, calorie restriction decreased bone formation rates at the periosteal and endosteal surfaces compared to HFD (Fig. 4). At the periosteal surface, mineralizing surface and mineral apposition rate were lower in HFD-CR mice compared to HFD in both sexes (Fig. 4A–B). In males, endocortical mineralizing surface was reduced in HFD-CR versus LFD (Fig. 4C). HFD-CR females had decreased endocortical mineralizing surface compared to their obese counterparts (Fig. 4D). Caloric restriction reduced endocortical mineral apposition rate in male HFD-CR versus HFD and LFD. Compared to LFD, calorie restriction decreased endocortical mineral apposition rate in females.

In male mice, trabecular bone formation rate was reduced in HFD-CR compared to HFD and LFD mice (Fig. 4E). Trabecular bone formation rates were lower in HFD-CR versus LFD females (Fig. 4F). In both sexes, trabecular mineralizing surface was not altered by diet. Compared to LFD and HFD mice, calorie restriction reduced trabecular mineral apposition rate in males. Trabecular mineral apposition rate did not differ by diet in female mice.

Serum P1NP, indicative of systemic bone formation, was lower in HFD-CR mice compared to controls in both male and female mice (Fig. 5A). Caloric restriction reduced systemic bone resorption, evaluated with serum CTx, in females but not males (Fig. 5B). Compared to control animals, caloric restriction decreased the number of osteoblasts per bone surface in trabecular bone in both male and female mice

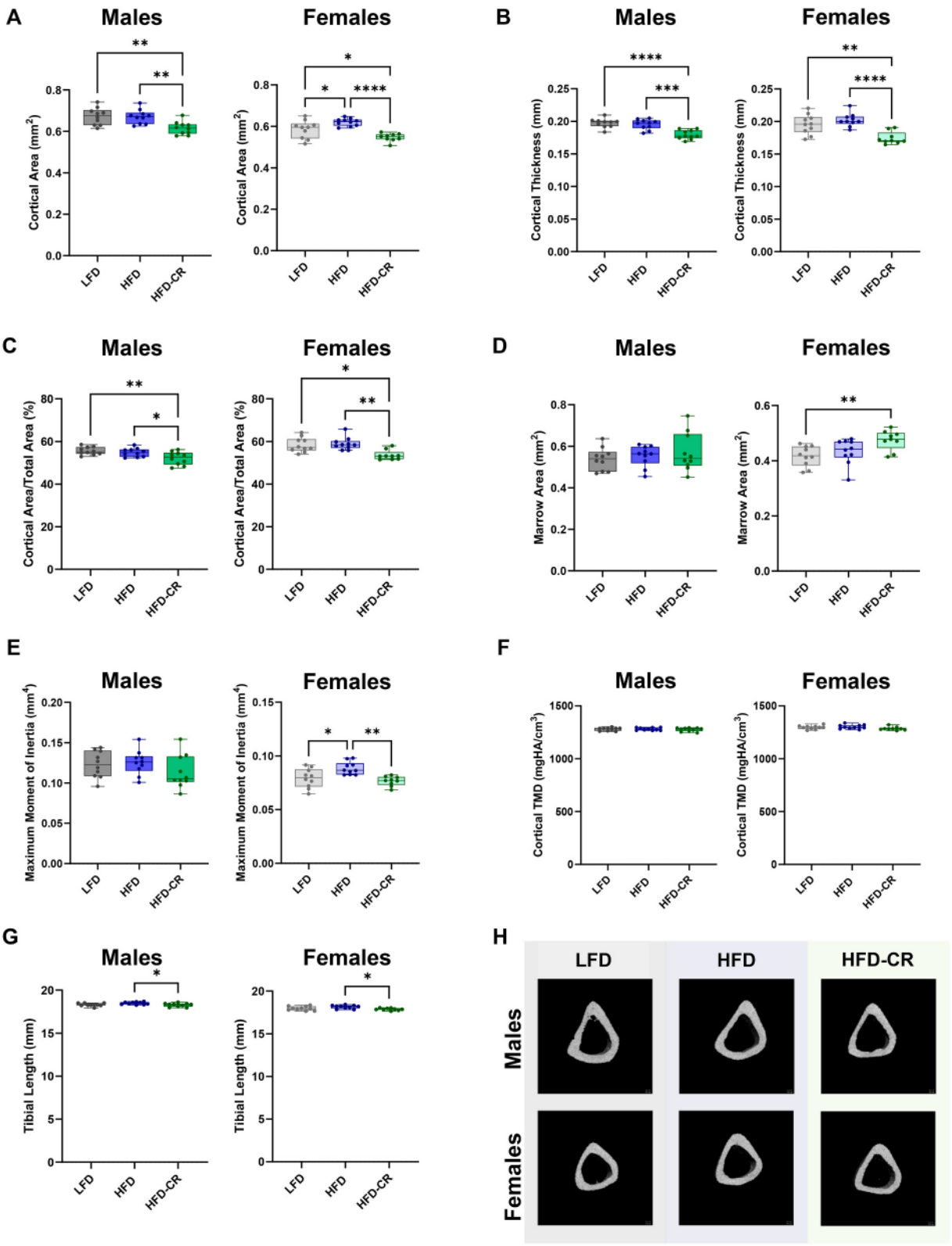


Fig. 2. Caloric restriction reduced cortical bone mass in previously obese mice. μCT was used to evaluate cortical bone morphology at the mid-diaphysis. (A) In both male and female mice, calorie restriction reduced cortical area compared to HFD. (B–C) Calorie restriction reduced both cortical thickness and cortical area fraction in both sexes. (D) In females, calorie restriction increased marrow area. Diet did not significantly alter marrow area in males. (E) Compared to their HFD counterparts, calorie restricted females had reduced maximum moment of inertia. Moment of inertia was not different by diet in males. (F) Diet did not change cortical tissue mineral density. (G) Calorie restricted mice had shorter tibiae compared to HFD animals. (H) Representative μCT images. Cortical bone morphology was evaluated by one-way ANOVA with factor of diet. Tukey post-hoc analysis determined differences between groups. Residuals were evaluated for normality using the Shapiro-Wilk test; data that was not normally distributed (Males: BV/TV) was evaluated with Kruskal-Wallis tests followed by Dunn's multiple comparisons test. $p \leq 0.05$ for all effects displayed. * indicates $p \leq 0.05$. ** indicates $p \leq 0.01$. *** indicates $p \leq 0.001$. **** indicates $p \leq 0.0001$.

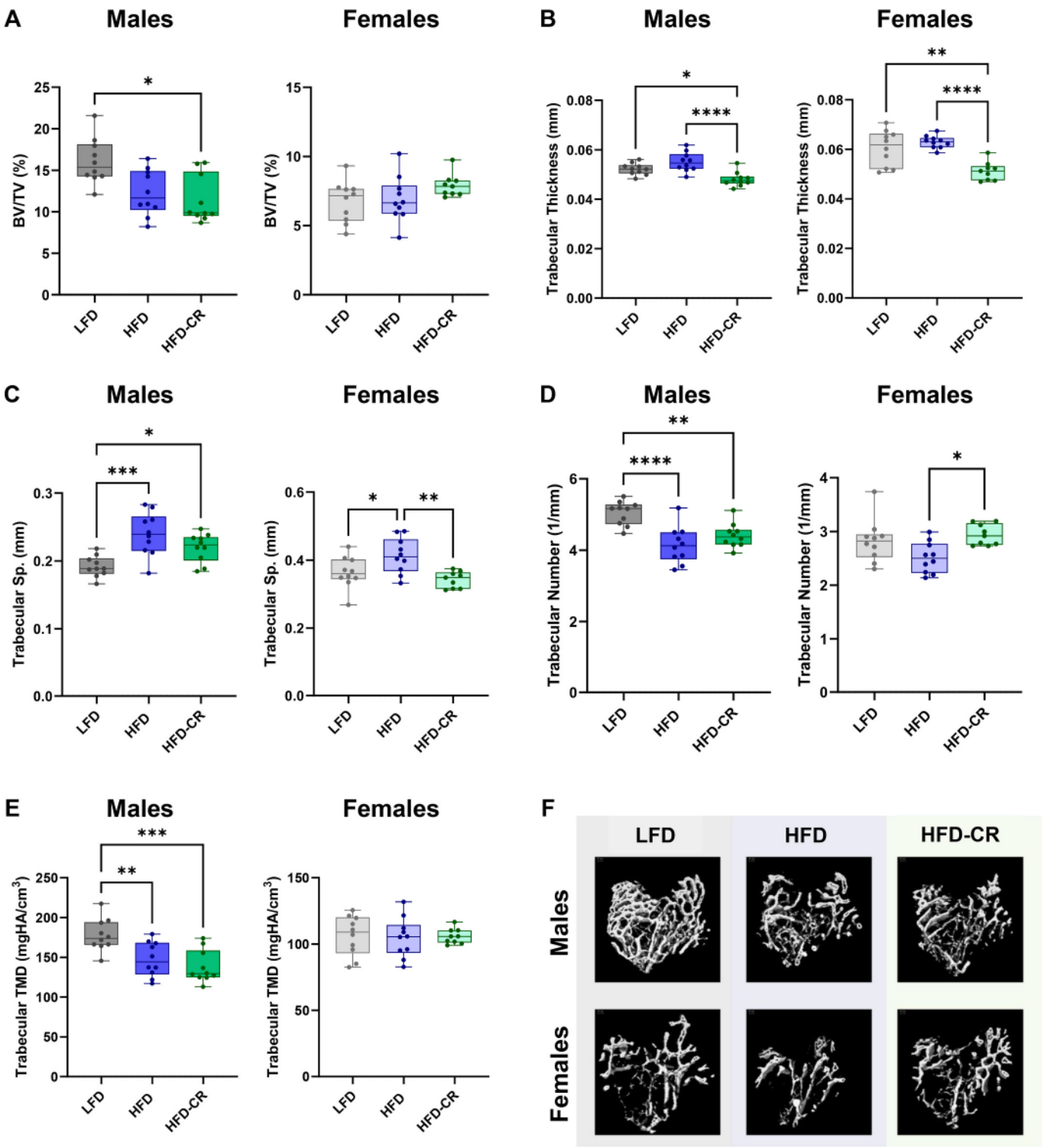


Fig. 3. Obesity and subsequent caloric restriction reduced trabecular bone mass. μCT was used to evaluate trabecular bone morphology. (A) In male mice, bone volume fraction was reduced in both HFD and HFD-CR animals. Bone volume fraction was not different by diet in female mice. (B) Compared to HFD, calorie restriction reduced trabecular thickness in both sexes. (C) HFD increased trabecular separation in both male and female mice. In females, subsequent caloric restriction increased trabecular spacing compared to HFD mice. (D) In male mice, both HFD and HFD-CR reduced trabecular number. Compared to HFD, HFD-CR increased trabecular number in females. (E) Trabecular tissue mineral density was reduced in both HFD and HFD-CR males but not different in females. (F) Representative μCT images. Trabecular bone morphology was evaluated by one-way ANOVA with factor of diet. Tukey post-hoc analysis determined differences between groups. Residuals were evaluated for normality using the Shapiro-Wilk test; data that was not normally distributed (Females: Cortical Area/Total Area, Marrow Area) was evaluated with Kruskal-Wallis tests followed by Dunn's multiple comparisons test. $p \leq 0.05$ for all effects displayed. * indicates $p \leq 0.05$. ** indicates $p \leq 0.01$. *** indicates $p \leq 0.001$. **** indicates $p \leq 0.0001$.

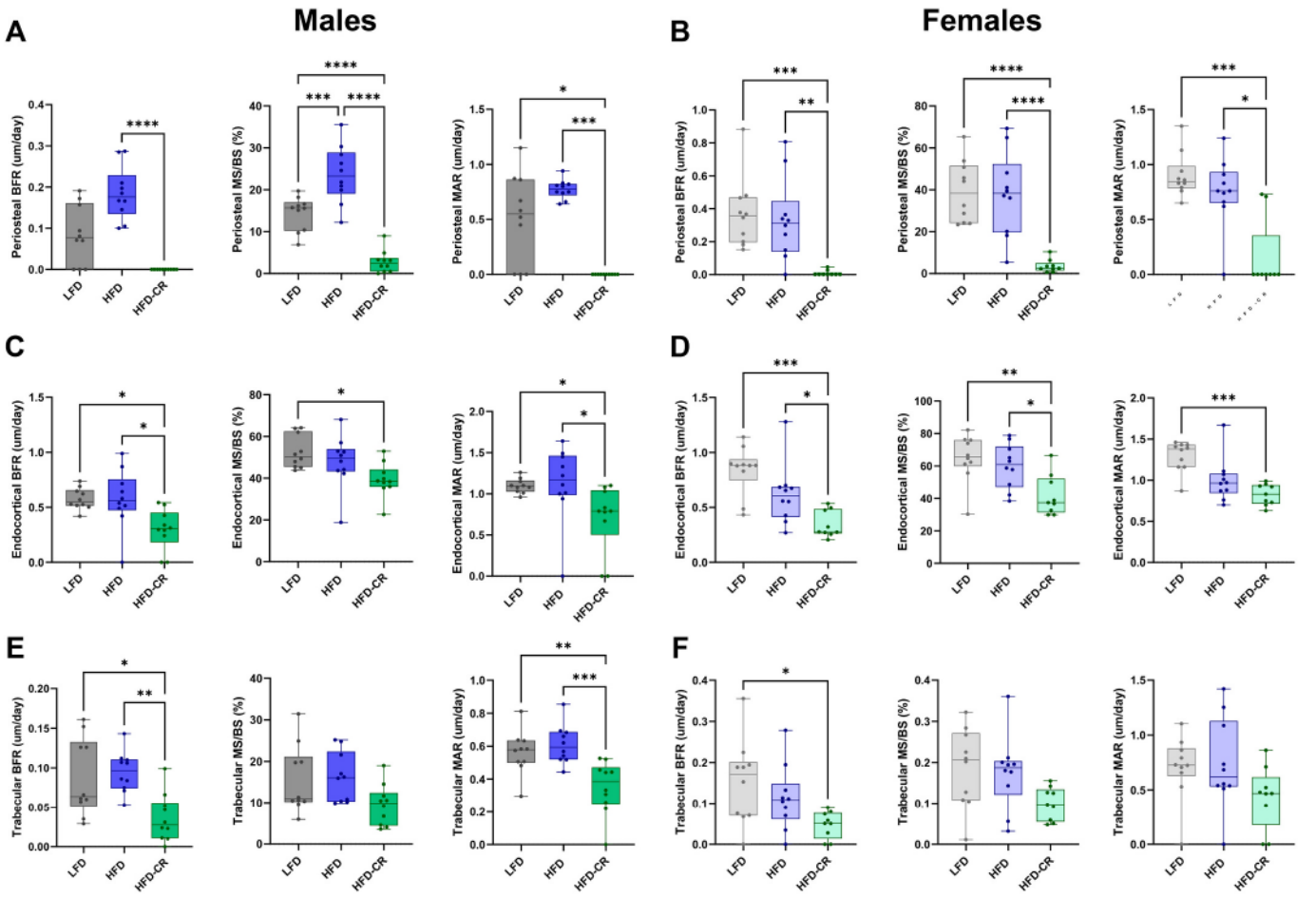


Fig. 4. Calorie restriction after obesity reduced bone formation rates. Dynamic histomorphometry was used to evaluate bone formation in cortical and trabecular bone. (A–B) Compared to HFD, calorie restriction reduced bone formation rate, mineralizing surface, and mineral apposition rate at the periosteal surface in both male and female mice. (C–D) At the endosteal surface, bone formation rate was lower in HFD-CR compared to HFD mice in both sexes. In males, endosteal mineralizing surface was lower in HFD-CR versus LFD mice. Compared to HFD, calorie restriction reduced mineral apposition rate males. In females, calorie restriction reduced endosteal mineralizing surface compared to both LFD and HFD mice. Both HFD and HFD-CR females had lower endosteal mineral apposition rates compared to LFD. (E) In males, caloric restriction reduced trabecular bone formation rate and mineral apposition rate compared to both HFD and LFD. Trabecular mineralizing surface was not different across diets in male mice. (F) Compared to LFD, HFD-CR reduced trabecular bone formation rate in female mice. Diet did not change trabecular mineralizing surface or mineral apposition rates in females. Bone formation rate, mineralizing surface, and mineral apposition rate were evaluated by one-way ANOVA with factor of diet. Tukey post-hoc analysis determined differences between groups. Residuals were evaluated for normality using the Shapiro-Wilk test; data that was not normally distributed (Males: Periosteal BFR, Periosteal MAR, Endosteal MAR, Trabecular MS/BS. Females: Periosteal BFR, Periosteal MAR, Endosteal MAR.) was evaluated with Kruskal-Wallis tests followed by Dunn's multiple comparisons test. $p \leq 0.05$ for all effects displayed. * indicates $p \leq 0.05$. ** indicates $p \leq 0.01$. *** indicates $p \leq 0.001$. **** indicates $p \leq 0.0001$.

(Fig. 5C–D). Compared to HFD mice, both LFD and HFD-CR females had fewer procollagen-1-stained cells on the trabecular bone surface (Fig. 5D). Osteoblast number was not changed by diet at the cortical surface (Fig. 5E). In males, the number of TRAP+ cells did not differ between diet groups (Fig. 5F–G). Compared to LFD, HFD and HFD-CR females had fewer TRAP-positive stained cells on the trabecular bone surface (Fig. 5F).

3.6. Diet shifted the cortical metabolome in sex-specific manners

Both high-fat diet and calorie restriction altered the cortical bone metabolome. In both sexes, the metabolome of HFD mice was distinct from LFD, with minimal overlap between groups (Fig. S2). HFD-CR further shifted the metabolome away from LFD in both male and female mice. Specific pathways responsible for the diet-induced metabolomic differences were distinct between male and female mice. Median metabolite intensity was normalized to controls, revealing metabolic changes induced by HFD and HFD-CR in cortical bone (Fig. 6). Clustering revealed that obesity (HFD) and subsequent weight loss (HFD-CR) distinctly affected the cortical metabolome compared to LFD mice. Pathways altered by diet generally mapped to amino acid or fatty acid metabolism.

To evaluate the specific changes to metabolic pathways identified, both HFD and HFD-CR were compared to LFD controls, and the pathways were then defined as up- or downregulated. In some clusters, directionality of HFD and HFD-CR was similar whereas other clusters demonstrated distinct changes following obesity or weight loss. In males, compared to LFD controls, most metabolic pathways identified were downregulated with HFD, HFD-CR, or in both groups. HFD reduced specific metabolic pathways that remained downregulated during subsequent caloric restriction; specifically, lysine degradation, arginine biosynthesis, arginine and proline metabolism, histidine metabolism, and glycerophospholipid metabolism, valine, leucine and isoleucine biosynthesis were downregulated in HFD and HFD-CR males compared to LFD controls. Compared to LFD, HFD males also had reduction of metabolic pathways that were generally not altered in HFD-CR mice, including glycine, serine, and threonine metabolism, phenylalanine metabolism, and nicotinate and nicotinamide metabolism. In

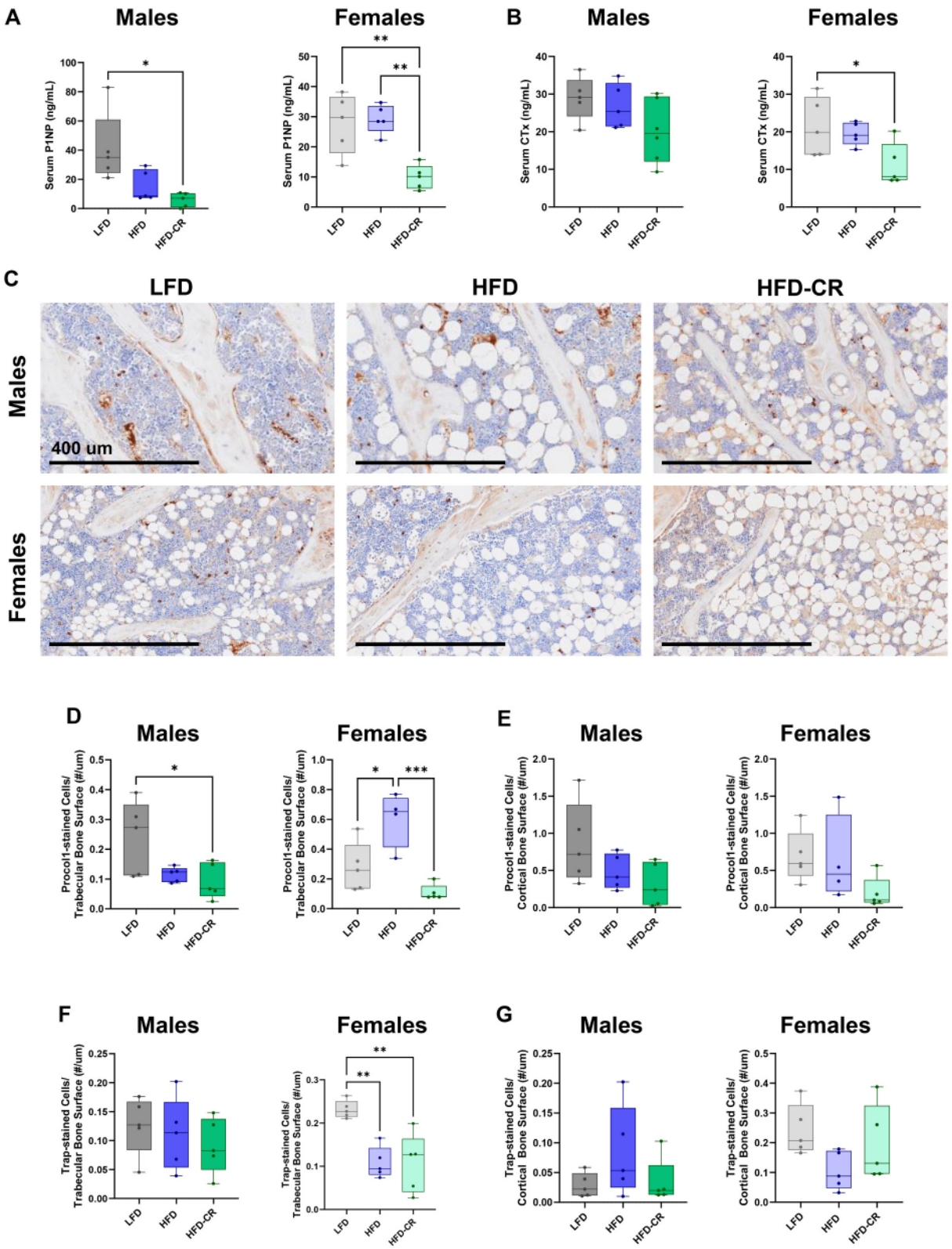


Fig. 5. Calorie restriction reduced systemic bone formation and resorption. Serum collected at euthanasia was used to evaluate systemic bone formation and resorption with P1NP and CTx, respectively. (A) In male mice, HFD-CR reduced P1NP versus LFD. Compared to both LFD and HFD, caloric restriction reduced P1NP in female mice. (B) Diet did not change CTx in males. In females, HFD-CR reduced CTx compared to LFD mice. (C) Representative images of trabecular bone stained with procollagen-1 (brown). Scale bar = 400 um. Osteoblast number, normalized to bone surface, was reduced in HFD-CR compared to LFD mice. P1NP, CTx, and osteoblast number were evaluated by one-way ANOVA with factor of diet. Tukey post-hoc analysis determined differences between groups. Residuals were evaluated for normality using the Shapiro-Wilk test; data that was not normally distributed (Males: P1NP. Females: Procol-1 stained cells/cortical bone surface) was evaluated with Kruskal-Wallis tests followed by Dunn's multiple comparisons test. $p \leq 0.05$ for all effects displayed. * indicates $p \leq 0.05$. ** indicates $p \leq 0.01$. *** indicates $p \leq 0.001$. (For interpretation of the references to colour in this figure legend, the reader is referred to the web version of this article.)

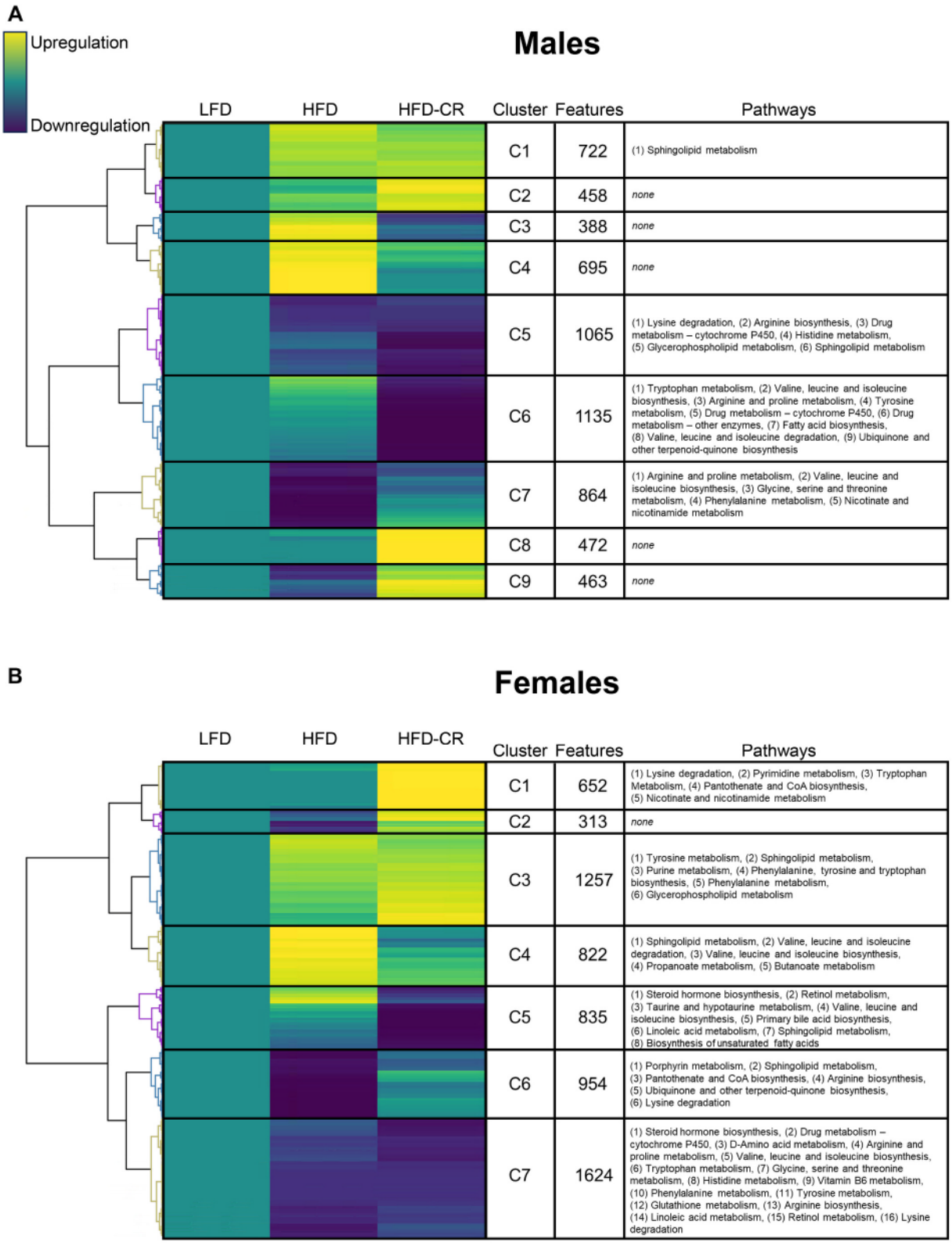


Fig. 6. Cortical bone metabolome was altered by diet in a sex-dependent manner. Metabolites were extracted from cortical bone and untargeted metabolomics performed. Within each diet group, the median intensity of individual metabolites was calculated and normalized to the control group (LFD). Normalized intensities were hierarchically clustered. Each cluster was then correlated to pathways associated with individual metabolites. For both (A) male and (B) female mice, compared to LFD controls, yellow indicates upregulation of identified metabolites, teal indicates no difference from LFD, and blue indicates downregulation. The number of metabolites within each cluster was quantified (Features). Pathways related to clustered metabolites revealed that diet shifted the cortical bone metabolome in a sex-dependent manner. (For interpretation of the references to colour in this figure legend, the reader is referred to the web version of this article.)

males, HFD-CR, but not HFD, was associated with a downregulation of pathways related to tryptophan metabolism, tyrosine metabolism, ubiquinone and other terpenoid-quinone biosynthesis, valine, leucine and isoleucine degradation, and fatty acid biosynthesis.

In females, metabolic pathways were both up- and downregulated by dietary interventions. Many of the metabolic pathways shared by HFD and HFD-CR females were downregulated compared to LFD controls, including steroid hormone biosynthesis, D-Amino acid metabolism, arginine and proline metabolism, glycine serine and threonine metabolism, histidine metabolism, vitamin B6 metabolism, glutathione metabolism, arginine biosynthesis, linoleic acid metabolism, and retinol metabolism. The upregulation of some metabolic pathways by HFD were also upregulated in HFD-CR females, including purine metabolism, glycerophospholipid metabolism, and phenylalanine tyrosine and tryptophan biosynthesis. HFD-induced increases in propanoate metabolism, butanoate metabolism, and valine, leucine, and isoleucine degradation were not present in HFD-CR females. Similarly, HFD-induced decreases in porphyrin metabolism, and ubiquinone and other terpenoid-quinone biosynthesis were not recorded in HFD-CR females. Pantothenate and CoA biosynthesis were decreased in HFD mice but increased in HFD-CR females. Although not changed by HFD, HFD-CR females had increased pyrimidine metabolism and nicotinate and nicotinamide metabolism. Similarly, HFD-CR decreased taurine and hypotaurine metabolism, primary bile acid biosynthesis, and biosynthesis of fatty acids but these pathways were not changed by HFD.

4. Discussion

Given the extent of the ongoing obesity epidemic, improved understanding of the effect of weight loss interventions on the skeleton are necessary. We demonstrated that in obese preclinical models, caloric restriction improved whole-body metabolism but further exacerbated bone loss. Reductions in bone formation and osteoblast number are likely responsible for diminished bone mass in calorie-restricted animals. In a sex-dependent manner, obesity and subsequent caloric restriction shifted the cortical bone metabolome, highlighting distinct changes to cellular metabolism within the skeleton in male and female mice.

Bone loss during weight loss cannot be fully attributed to mechanoadaptation; although the reductions in bodyweight decrease the load on the skeleton, previous research has established that mechanoadaptation is diminished during weight loss in both humans and mice. In young, healthy humans and mice, mechanical loading of the skeleton stimulates anabolic activity [37,38]. The ability to respond to mechanical loading is diminished during weight loss; in mice, increasing exercise through the addition of running wheels during the diet period did not prevent calorie restriction-induced bone loss in nonobese mice [39]. In our study, the increased ambulatory activity of the calorie-restricted mice did not prevent bone loss. Similarly, in humans, resistance training interventions during weight loss are not sufficient to maintain bone mass. Resistance training, but not aerobic exercise, attenuated bone loss in obese or overweight humans during five months of calorie restriction [40]; however, during longer periods of calorie restriction (12 months), bone loss at the hip occurred in participants, regardless of resistance training intervention [41]. Although initial losses in bone mass may be attributable to reductions in bodyweight, the lack of mechanoresponsiveness of the skeleton following longer periods of caloric restriction suggests distinct mechanisms for bone loss. In our study, compared to control animals, calorie restricted mice had more distinct differences in the cortical metabolome than their obese counterparts; should mechanoadaptation explain the bone loss during weight loss, we would expect to measure more similarities between control and calorie-restricted animals, despite differences in their bodyweights at euthanasia. Concurrent anabolic interventions may prevent bone loss during caloric restriction. Although the addition of mechanical loading during weight loss does not elicit anabolic responses of the skeleton in humans or mice, in nonobese mice, simultaneous treatment with parathyroid hormone during caloric restriction attenuated trabecular bone loss [20]. Parathyroid hormone elicits changes to cellular metabolism within bone that are necessary for its anabolic effects [42,43]. The changes we identified in the cortical bone metabolome following obesity and weight loss provide key insights into novel, future interventions.

The changes in metabolism of bone cells during obesity and subsequent weight loss likely drive the morphological changes recorded in our study, and highlight the importance of evaluating both male and female mice separately. The sex-specific responses of the cortical metabolome to dietary interventions reported here build on previous work, which established sexually dimorphic metabotypes in cortical bone [36]. In our study, within the cortical bone of male mice, caloric restriction after obesity reduced tryptophan metabolism, which has previously been linked to bone loss [44]. In females, the calorie restriction-induced downregulation of pathways related to taurine metabolism likely reflects altered osteocyte metabolism; taurine is a metabolite produced by osteocytes that positively regulates bone formation [45]. In both male and female mice, caloric restriction after obesity decreased fatty acid biosynthesis, which may have directly contributed to the reductions in osteoblast activity. Fatty acids are critical for osteoblast function, especially during nutrient limitation [46]. Notably, specific weight loss strategies may elicit distinct changes to the metabolism within the bone; treatment with the SGLT2 inhibitor canagliflozin also causes weight loss, but within cortical bone, tryptophan catabolism was increased [47]. Additionally, the metabolites measured in our osteocyte-enriched samples could reflect metabolism of other bone cells. Although our removal of the periosteum and centrifugation of the marrow reduces potential contributions of metabolites contained within the bone lining or marrow-resident cells, metabolite trafficking prior to euthanasia could contribute to the cortical metabolome we evaluated.

Different clinical strategies for weight loss may cause distinct changes to the skeleton. These interventions range from lifestyle changes to anti-obesity medications, and even surgical options. Although lifestyle interventions are the first-line clinical recommendations for weight loss, humans losing weight through diet and exercise typically regain weight after the intervention period [48]. The recent revolution in anti-obesity medications has expanded weight loss options for patients. Glucagon-like peptide-1 receptor agonists reduce appetite and food intake, thereby eliciting weight loss [49]. Early clinical data suggest that semaglutide causes cortical bone loss in humans [50]. For individuals who do not achieve weight loss with lifestyle interventions, anti-obesity medications may offer more skeletal protection compared to surgical interventions; bariatric surgery has well-established negative effects on bone in both humans [51,52] and mouse models [53,54], with preclinical studies demonstrating that bariatric surgery elicits more bone loss than anti-obesity medications [55]. Future work should evaluate potential differences in the skeleton following weight loss with caloric restriction versus therapeutic interventions.

Weight loss via caloric restriction versus the return to a normal diet elicits differential changes to the skeleton. We established that the cortical metabolome of calorie-restricted mice was distinct from the LFD control animals, suggesting that weight loss does not return the skeleton to normal metabolomic conditions. Further, in our study, caloric restriction reduced trabecular and cortical bone mass in both sexes whereas weight loss through the return to a normal diet altered bone morphology in a sex-dependent manner [9,27]. Previous work established that obese male mice returned to a normal chow diet had improved trabecular bone mass and similar cortical bone strength [9]. On the other hand, compared to lifelong obese mice, females returned to a normal diet retained obesity-induced trabecular deficits but had improved cortical bone strength [27]. After the return to a normal diet, the body mass of formerly obese mice was similar to controls [9,27]. Differences in composition of control diets may influence our ability to identify skeletal changes following weight loss; compared to standard

chow diets, low fat diets are high in carbohydrate content and may exacerbate age-related bone loss [32]. Despite the potential for reduced bone mass in our control group, the use of sucrose-matched low fat diets are preferable when studying obesity [56]. Sucrose influences whole body metabolism and thus diets not matched in sucrose would introduce additional confounding variables [56]. In our study, in obese animals, consumption of the low-fat control diet for the short period of two weeks reduced body mass, but subsequent calorie restriction elicited more weight loss, decreasing bodyweights below that of control groups. Most animals tolerated these dietary changes and rapid weight loss, thus diminishing the need for a Stabilization Phase in future studies.

Future work should address the limitations of our research. Individual bone cells rely on specific bioenergetic programs [57]. Although the cortical sample used for metabolomic analysis in this study was likely composed primarily of bone-resident osteocytes, we were unable to assign metabolites to specific cell types. Further, cortical and trabecular bone have distinct transcriptional signatures [58,59] and also rely on different bioenergetic programs [60]. Although we identified calorie restriction-induced deficits in bone morphology and bone formation, we did not directly evaluate bone strength. The translation of bone loss to increased fracture risk should be confirmed in future studies. Additionally, the contributions mechanoadaptation versus weight loss should be dissected in future research; in our study, calorie-restricted animals weighed less than control mice at euthanasia, precluding us from directly separating these effects. Bone marrow adiposity also has been linked to overall skeletal health [61]. We measured increased bone marrow adiposity due to obesity and subsequent caloric restriction, but our small sample size may have precluded us from identifying any synergistic effects of weight loss after obesity. Future work should also investigate changes to signaling pathways within bone marrow adipocytes following weight loss [62]. Similarly, our small sample sizes used for histology and for confirming obesity-induced deficits in bone mass and formation prior to weight loss could have precluded us from identifying additional differences between groups. Finally, the data collected during in vivo dual-energy x-ray absorptiometry scans may be influenced by animal or bone size [25], therefore future investigations would be strengthened by the use of in vivo micro-computed tomography.

This research establishes that caloric restriction after obesity reduces bone mass and shifts the cortical metabolome. We determined that in both male and female mice, caloric restriction reduced cortical bone mass and trabecular thickness. Notably, the cortical bone metabolome was changed in obese mice compared to control animals, but further shifted by subsequent caloric restriction. Diet-induced metabolic shifts were sex-specific, highlighting the potential for distinct mechanisms to contribute to calorie restriction-induced bone loss in male versus female mice. Importantly, this work highlights potential clinical concerns surrounding weight loss after obesity; although calorie restriction may improve whole body metabolic outcomes, fracture risk will likely increase.

CRediT authorship contribution statement

Carolyn Chlebek: Writing – review & editing, Writing – original draft, Visualization, Validation, Supervision, Software, Resources, Project administration, Methodology, Investigation, Funding acquisition, Formal analysis, Data curation, Conceptualization. **Casey McAndrews:** Writing – review & editing, Validation, Investigation, Funding acquisition, Formal analysis, Data curation. **Benjamin Aaronson:** Writing – review & editing, Visualization, Validation, Investigation, Funding acquisition, Formal analysis, Data curation. **Hope D. Welhaven:** Writing – review & editing, Visualization, Validation, Software, Methodology, Investigation, Formal analysis, Data curation. **Kanglun Yu:** Writing – review & editing, Investigation, Formal analysis, Data curation. **Samantha N. Costa:** Writing – review & editing, Validation, Methodology, Investigation, Formal analysis, Data curation. **Joseph Shaver:** Writing – review & editing, Investigation, Formal analysis. **Sophia Silvia:** Writing – review & editing, Validation, Investigation, Formal analysis, Data curation. **Victoria E. DeMambro:** Writing – review & editing, Formal analysis. **Ronald K. June:** Writing – review & editing, Supervision, Software, Resources, Methodology, Funding acquisition. **Meghan E. McGee-Lawrence:** Writing – review & editing, Supervision, Software, Resources, Funding acquisition, Formal analysis. **Clifford J. Rosen:** Writing – review & editing, Supervision, Software, Resources, Project administration, Methodology, Funding acquisition, Conceptualization.

Ethics approval/institutional review board statement

The animal study protocol was approved by the Institutional Animal Care and Use Committee (IACUC) of MaineHealth Institute for Research (protocol #2209).

Funding

This work was supported by the Stryker/ORS Women's Research Fellowship, a grant from Stryker administered by the Orthopaedic Research Society (CC). CM was supported by the Endocrine Society Research Experiences for Graduate and Medical Students. BA was supported by the University of New England Carmen Pettapiece Student Research Fellowship. DXA scans and indirect calorimetry were supported by the services of the Physiology Core of the COBRE in Mesenchymal and Neural Regulation of Metabolic Networks (2P20GM121301). Histology was performed at the University of New England Histology and Imaging Core, funded by NIGMS P20GM103643. Dynamic histomorphometry was performed by the Functional Outcomes Core (Core B) at Augusta University, funded by NIA P01 AG036675 with the support of the Augusta University Medical College of Georgia Electron Microscopy and Histology Core Facility, RRID:SCR_026810. Metabolomics was performed at the Montana State Mass Spectrometry Facility (RRID:SCR_012482), made possible in part by the MJ Murdock Charitable Trust, the National Institute of General Medical Sciences of the National Institutes of Health (P20GM103474 and S10OD28650), and the MSU Office of Research and Economic Development.

Declaration of competing interest

The authors declare no conflict of interest. All authors have read and agreed to the published version of the manuscript.

Acknowledgements

We thank Peter Caradonna for assistance with histology and Jen Daruszka for assistance with animal work.

Appendix A. Supplementary data

Supplementary data to this article can be found online at https://doi.org/10.1016/j.bone.2025.117690.

Data availability

Metabolomics data will be uploaded to Metabolomics Workbench upon acceptance.

References

[1] J. Kessler, C. Koebnick, N. Smith, A. Adams, Childhood obesity is associated with increased risk of most lower extremity fractures, Clin. Orthop. 471 (4) (Apr. 2013) 1199–1207, https://doi.org/10.1007/s11999-012-2621-z.

[2] A.-F. Turcotte, et al., Association between obesity and risk of fracture, bone mineral density and bone quality in adults: a systematic review and meta-analysis, PLoS

One 16 (6) (June 2021) e0252487, https://doi.org/10.1371/journal.pone.0252487.
[3] Y. Wang, M.A. Beydoun, J. Min, H. Xue, L.A. Kaminsky, L.J. Cheskin, Has the prevalence of overweight, obesity and central obesity levelled off in the United States? Trends, patterns, disparities, and future projections for the obesity epidemic, Int. J. Epidemiol. 49 (3) (June 2020) 810–823, https://doi.org/10.1093/ije/dyz273.
[4] L.M. March, H. Bagga, Epidemiology of osteoarthritis in Australia, Med. J. Aust. 180 (S5) (Mar. 2004), https://doi.org/10.5694/j.1326-5377.2004.tb05906.x.
[5] D. Botticelli, N.P. Lang, Dynamics of osseointegration in various human and animal models - a comparative analysis, Clin. Oral Implants Res. 28 (6) (June 2017) 742–748, https://doi.org/10.1111/clr.12872.
[6] K.M. Gadde, C.K. Martin, H.-R. Berthoud, S.B. Heymsfield, Obesity: pathophysiology and management, J. Am. Coll. Cardiol. 71 (1) (Jan. 2018) 69–84, https://doi.org/10.1016/j.jacc.2017.11.011.
[7] M. Tencerova, F. Figeac, N. Ditzel, H. Taipaleenmäki, T.K. Nielsen, M. Kassem, High-Fat Diet-Induced Obesity Promotes Expansion of Bone Marrow Adipose Tissue and Impairs Skeletal Stem Cell Functions in Mice, J. Bone Miner. Res. 33 (6) (June 2018) 1154–1165, https://doi.org/10.1002/jbmr.3408.
[8] D. Ross, et al., Distinct effects of a high fat diet on bone in skeletally mature and developing male C57BL/6J mice, Nutrients 13 (5) (May 2021) 1666, https://doi.org/10.3390/nu13051666.
[9] E.L. Scheller, et al., Changes in skeletal integrity and marrow adiposity during high-fat diet and after weight loss, Front. Endocrinol. 7 (July 2016), https://doi.org/10.3389/fendo.2016.00102.
[10] A. Gandham, et al., Associations of body mass index, body fat percentage and sarcopenia components with bone health estimated by second-generation high-resolution peripheral quantitative computed tomography in older adults with obesity, Exp. Gerontol. 179 (Aug. 2023) 112227, https://doi.org/10.1016/j.exger.2023.112227.
[11] M.A. Bredella, et al., Determinants of bone microarchitecture and mechanical properties in obese men, J. Clin. Endocrinol. Metab. 97 (11) (Nov. 2012) 4115–4122, https://doi.org/10.1210/jc.2012-2246.
[12] M.A. Bredella, et al., Vertebral bone marrow fat is positively associated with visceral fat and inversely associated with IGF-1 in obese women, Obesity 19 (1) (Jan. 2011) 49–53, https://doi.org/10.1038/oby.2010.106.
[13] P.K. Fazeli, et al., Marrow fat and bone—new perspectives, J. Clin. Endocrinol. Metab. 98 (3) (Mar. 2013) 935–945, https://doi.org/10.1210/jc.2012-3634.
[14] D.T. Villareal, Bone mineral density response to caloric restriction–induced weight loss or exercise-induced weight loss: a randomized controlled trial, Arch. Intern. Med. 166 (22) (Dec. 2006) 2502, https://doi.org/10.1001/archinte.166.22.2502.
[15] D.T. Villareal, et al., Effect of two-year caloric restriction on bone metabolism and bone mineral density in non-obese younger adults: a randomized clinical trial, J. Bone Miner. Res. 31 (1) (Jan. 2016) 40–51, https://doi.org/10.1002/jbmr.2701.
[16] F. Johannesdottir, M.S. Putman, S.-A.M. Burnett-Bowie, J.S. Finkelstein, E.W. Yu, M.L. Bouxsein, Age-related changes in bone density, microarchitecture, and strength in postmenopausal black and white women: the SWAN Longitudinal HR-pQCT study, J. Bone Miner. Res. 37 (1) (Dec. 2020) 41–51, https://doi.org/10.1002/jbmr.4460.
[17] L. Louvet, et al., Sirtuin 1 deficiency decreases bone mass and increases bone marrow adiposity in a mouse model of chronic energy deficiency, Bone 136 (July 2020) 115361, https://doi.org/10.1016/j.bone.2020.115361.
[18] M.J. Devlin, et al., Caloric restriction leads to high marrow adiposity and low bone mass in growing mice, J. Bone Miner. Res. 25 (9) (Sept. 2010) 2078–2088, https://doi.org/10.1002/jbmr.82.
[19] M.W. Hamrick, K.-H. Ding, S. Ponnala, S.L. Ferrari, C.M. Isales, Caloric restriction decreases cortical bone mass but spares trabecular bone in the mouse skeleton: implications for the regulation of bone mass by body weight, J. Bone Miner. Res. 23 (6) (Feb. 2008) 870–878, https://doi.org/10.1359/jbmr.080213.
[20] D.E. Maridas, et al., Progenitor recruitment and adipogenic lipolysis contribute to the anabolic actions of parathyroid hormone on the skeleton, FASEB J. 33 (2) (Feb. 2019) 2885–2898, https://doi.org/10.1096/fj.201800948RR.
[21] L. Liu, et al., Calorie restriction in mice impairs cortical but not trabecular peak bone mass by suppressing bone remodeling, J. Bone Miner. Res. (July 2024) zjae104, https://doi.org/10.1093/jbmr/zjae104.
[22] M.A. Bredella, et al., Increased bone marrow fat in anorexia nervosa, J. Clin. Endocrinol. Metab. 94 (6) (June 2009) 2129–2136, https://doi.org/10.1210/jc.2008-2532.
[23] M.A. Bredella, et al., Bone marrow adipose tissue composition following high-caloric feeding and fasting, Bone 152 (Nov. 2021) 116093, https://doi.org/10.1016/j.bone.2021.116093.
[24] A. Tirosh, R.J. De Souza, F. Sacks, G.A. Bray, S.R. Smith, M.S. LeBoff, Sex differences in the effects of weight loss diets on bone mineral density and body composition: POUNDS LOST trial, J. Clin. Endocrinol. Metab. 100 (6) (2015) 2463–2471, https://doi.org/10.1210/jc.2015-1050.
[25] E.W. Yu, B.J. Thomas, J.K. Brown, J.S. Finkelstein, Simulated increases in body fat and errors in bone mineral density measurements by DXA and QCT, J. Bone Miner. Res. 27 (1) (Jan. 2012) 119–124, https://doi.org/10.1002/jbmr.506.
[26] L. Nelson, K.Y. Gulenchyn, M. Atthey, C.E. Webber, Is a fixed value for the least significant change appropriate? J. Clin. Densitom. 13 (1) (Jan. 2010) 18–23, https://doi.org/10.1016/j.jocd.2009.10.001.
[27] S. Ben Tahar, et al., Adolescent obesity incurs adult skeletal deficits in murine induced obesity model, J. Orthop. Res. (June 2022) jor.25378, https://doi.org/10.1002/jor.25378.
[28] A.-K. Picke, et al., Differential effects of high-fat diet and exercise training on bone and energy metabolism, Bone 116 (Nov. 2018) 120–134, https://doi.org/10.1016/j.bone.2018.07.015.
[29] A. Fogarasi, K. Gonzalez, M. Dalamaga, F. Magkos, The impact of the rate of weight loss on body composition and metabolism, Curr. Obes. Rep. 11 (2) (2022) 33–44, https://doi.org/10.1007/s13679-022-00470-4.
[30] H.D. Welhaven, A.H. Welfley, B. Bothner, S.P. Messier, R.F. Loeser, R.K. June, The metabolome of male and female individuals with knee osteoarthritis is influenced by 18-months of weight loss intervention: the IDEA trial, BMC Musculoskelet. Disord. 25 (1) (Dec. 2024) 1057, https://doi.org/10.1186/s12891-024-08166-7.
[31] C. Medeiros, J.M. Wallace, High glucose-induced inhibition of osteoblast like MC3T3-E1 differentiation promotes mitochondrial perturbations, PLoS One 17 (6) (June 2022) e0270001, https://doi.org/10.1371/journal.pone.0270001.
[32] N.S. Dole, et al., High-fat and high-carbohydrate diets increase bone fragility through TGF-β–dependent control of osteocyte function, JCI Insight 9 (16) (Aug. 2024) e175103, https://doi.org/10.1172/jci.insight.175103.
[33] V.E. DeMambro, et al., Igfbp2 deletion in ovariectomized mice enhances energy expenditure but accelerates bone loss, Endocrinology 156 (11) (Nov. 2015) 4129–4140, https://doi.org/10.1210/en.2014-1452.
[34] S. Costa, H. Fairfield, M.R. Reagan, Inverse correlation between trabecular bone volume and bone marrow adipose tissue in rats treated with osteoanabolic agents, Bone 123 (June 2019) 211–223, https://doi.org/10.1016/j.bone.2019.03.038.
[35] M.L. Bouxsein, S.K. Boyd, B.A. Christiansen, R.E. Guldberg, K.J. Jepsen, R. Müller, Guidelines for assessment of bone microstructure in rodents using micro–computed tomography, J. Bone Miner. Res. 25 (7) (July 2010) 1468–1486, https://doi.org/10.1002/jbmr.141.
[36] H.D. Welhaven, et al., The cortical bone metabolome of C57BL / 6J mice is sexually dimorphic, JBMR Plus 6 (7) (July 2022), https://doi.org/10.1002/jbm4.10654.
[37] C. Snow-Harter, M.L. Bouxsein, B.T. Lewis, D.R. Carter, R. Marcus, Effects of resistance and endurance exercise on bone mineral status of young women: a randomized exercise intervention trial, J. Bone Miner. Res. 7 (7) (Dec. 2009) 761–769, https://doi.org/10.1002/jbmr.5650070706.
[38] J. Fritton, E. Myers, T. Wright, M. van der Meulen, Loading induces site-specific increases in mineral content assessed by microcomputed tomography of the mouse tibia, Bone 36 (6) (June 2005) 1030–1038, https://doi.org/10.1016/j.bone.2005.02.013.
[39] C. McGrath, et al., Exercise degrades bone in caloric restriction, despite suppression of marrow adipose tissue (MAT), J. Bone Miner. Res. 35 (1) (Jan. 2020) 106–115, https://doi.org/10.1002/jbmr.3872.
[40] K.M. Beavers, et al., Change in bone mineral density during weight loss with resistance versus aerobic exercise training in older adults, J. Gerontol. Ser. A 72 (11) (2017) 1582–1585, https://doi.org/10.1093/gerona/glx048.
[41] K.M. Beavers, et al., Weighted vest use or resistance exercise to offset weight loss–associated bone loss in older adults: a randomized clinical trial, JAMA Netw. Open 8 (6) (June 2025) e2516772, https://doi.org/10.1001/jamanetworkopen.2025.16772.
[42] V.E. DeMambro, L. Tian, V. Karthik, C.J. Rosen, A.R. Guntur, Effects of PTH on osteoblast bioenergetics in response to glucose, Bone Rep. 19 (Dec. 2023) 101705, https://doi.org/10.1016/j.bonr.2023.101705.
[43] S. Stegen, C. Devignes, S. Torrekens, R. Van Looveren, P. Carmeliet, G. Carmeliet, Glutamine metabolism in osteoprogenitors is required for bone mass accrual and PTH -induced bone anabolism in male mice, J. Bone Miner. Res. 36 (3) (Mar. 2021) 604–616, https://doi.org/10.1002/jbmr.4219.
[44] M.E. Refaey, et al., Kynurenine, a tryptophan metabolite that accumulates with age, induces bone loss, J. Bone Miner. Res. 32 (11) (Nov. 2017) 2182–2193, https://doi.org/10.1002/jbmr.3224.
[45] M. Prideaux, Y. Kitase, M. Kimble, T.M. O'Connell, L.F. Bonewald, Taurine, an osteocyte metabolite, protects against oxidative stress-induced cell death and decreases inhibitors of the Wnt/β-catenin signaling pathway, Bone 137 (Aug. 2020) 115374, https://doi.org/10.1016/j.bone.2020.115374.
[46] A. Nandy, et al., Lipolysis supports bone formation by providing osteoblasts with endogenous fatty acid substrates to maintain bioenergetic status, Bone Res. 11 (1) (Nov. 2023) 62, https://doi.org/10.1038/s41413-023-00297-2.
[47] S.B. Poudel, et al., Canagliflozin-induced adaptive metabolism in bone, Diabetes (Feb. 2025) db240955, https://doi.org/10.2337/db24-0955.
[48] J.W. Anderson, E.C. Konz, R.C. Frederich, C.L. Wood, Long-term weight-loss maintenance: a meta-analysis of US studies, Am. J. Clin. Nutr. 74 (5) (Nov. 2001) 579–584, https://doi.org/10.1093/ajcn/74.5.579.
[49] S. Gabery, et al., Semaglutide lowers body weight in rodents via distributed neural pathways, JCI Insight 5 (6) (Mar. 2020) e133429, https://doi.org/10.1172/jci.insight.133429.
[50] M.S. Hansen, et al., Once-weekly semaglutide versus placebo in adults with increased fracture risk: a randomised, double-blinded, two-centre, phase 2 trial, eClinicalMedicine 72 (June 2024) 102624, https://doi.org/10.1016/j.eclinm.2024.102624.
[51] M.A. Bredella, et al., Impact of sleeve gastrectomy on bone outcomes in adolescents vs. adults with obesity, Bone 149 (Aug. 2021) 115975, https://doi.org/10.1016/j.bone.2021.115975.
[52] E.M. Stein, S.J. Silverberg, Bone loss after bariatric surgery: causes, consequences, and management, Lancet Diabetes Endocrinol. 2 (2) (Feb. 2014) 165–174, https://doi.org/10.1016/S2213-8587(13)70183-9.
[53] Z. Li, et al., G-CSF partially mediates effects of sleeve gastrectomy on the bone marrow niche, J. Clin. Invest. 129 (6) (May 2019) 2404–2416, https://doi.org/10.1172/JCI126173.
[54] K. Corbeels, et al., The curious fate of bone following bariatric surgery: bone effects of sleeve gastrectomy (SG) and Roux-en-Y gastric bypass (RYGB) in mice, Int. J.

Obes. 44 (10) (Oct. 2020) 2165–2176, https://doi.org/10.1038/s41366-020-0626-3.
[55] C.D.C. Picoli, et al., Vertical sleeve gastrectomy and semaglutide have distinct effects on skeletal health and heart function in obese male mice, Am. J. Physiol.-Endocrinol. Metab. (Mar. 2025), https://doi.org/10.1152/ajpendo.00521.2024 p. ajpendo.00521.2024.
[56] E. Rendina-Ruedy, B.J. Smith, Methodological considerations when studying the skeletal response to glucose intolerance using the diet-induced obesity model, BoneKEy Rep. 5 (Oct. 2016), https://doi.org/10.1038/bonekey.2016.71.
[57] R.C. Riddle, T.L. Clemens, Bone cell bioenergetics and skeletal energy homeostasis, Physiol. Rev. 97 (2) (Apr. 2017) 667–698, https://doi.org/10.1152/physrev.00022.2016.
[58] N.H. Kelly, J.C. Schimenti, F.P. Ross, M.C.H. van der Meulen, Transcriptional profiling of cortical versus cancellous bone from mechanically-loaded murine tibiae reveals differential gene expression, Bone 86 (May 2016) 22–29, https://doi.org/10.1016/j.bone.2016.02.007.
[59] C. Chlebek, M.S. Raynor, F.P. Ross, M.C.H. Van Der Meulen, The skeletal transcriptional response to mechanical load varies with age and tissue compartment in female mice, JBMR Plus (June 2025), https://doi.org/10.1093/jbmrpl/ziaf105.
[60] C. Chlebek, T.J. McNeill, M. Huang, M.S. Raynor, M.C.H. Van Der Meulen, Bioenergetic programs of cancellous and cortical bone are distinct and differ with age and mechanical loading, Sci. Rep. 15 (1) (May 2025) 19134, https://doi.org/10.1038/s41598-025-02141-5.
[61] M.J. Devlin, C.J. Rosen, The bone–fat interface: basic and clinical implications of marrow adiposity, Lancet Diabetes Endocrinol. 3 (2) (Feb. 2015) 141–147, https://doi.org/10.1016/S2213-8587(14)70007-5.
[62] S.N. Costa, et al., Altered metabolomics and inflammatory transcriptomics in human bone marrow adipocytes after acute high calorie diet and acute fasting, Front. Endocrinol. 16 (June 2025), https://doi.org/10.3389/fendo.2025.1591280.